Proc. Natl. Acad. Sci. USA
Vol. 79, pp. 2549–2553, April 1982
Biophysics

Junction between Z and B conformations in a DNA restriction fragment: Evaluation by Raman spectroscopy

(left- and right-handed duplexes/DNA distortion)

ROGER M. WARTELL*, JAN KLYSIK†, WOLFGANG HILLEN†‡, AND ROBERT D. WELLS†

*Schools of Physics and Biology, Georgia Institute of Technology, Atlanta, Georgia 30329; and †Department of Biochemistry, College of Agricultural and Life Sciences, University of Wisconsin, Madison, Wisconsin 53706

Communicated by Peter H. von Hippel, December 8, 1981

ABSTRACT **Raman vibrational spectra were obtained from two DNA restriction fragments and the DNA polymer (dG-dC)$_n$·(dG-dC)$_n$ in 0.01 and 4.5 M NaCl. One fragment contained 95 base pairs (bp) of the *Escherichia coli* lactose operator–promoter region (95-bp fragment). The other fragment consisted of the 95-bp region flanked by 26 and 32 bp of dC-dG sequences and *Bam*HI ends (157-bp fragment). In 0.01 M NaCl all three DNAs have Raman spectra characteristic of a right-handed B conformation. The high salt spectrum of the 95-bp fragment is also characteristic of a B conformation. However, the spectrum of the 157-bp fragment in 4.5 M NaCl shows major intensity changes from the 0.01 M NaCl spectrum. These changes are also observed in the high salt spectra of (dG-dC)$_n$·(dG-dC)$_n$ and are correlated with the presence of a left-handed Z conformation. Comparisons between the high salt Raman spectra of the 157-bp fragment and spectra calculated from (dG-dC)$_n$·(dG-dC)$_n$ and the 95-bp fragment indicated that essentially all of the dC-dG regions in the 157-bp fragment are in the Z conformation and a large part (≈80%) of the 95-bp region no longer has a B-type backbone vibration. However, this non-B-DNA-like character of the central region is not indicated by base vibrations.**

Repeating sequences of alternating dC and dG nucleotides can form left-handed duplex DNA conformations. This was demonstrated in the solid state by x-ray diffraction studies of crystals of d(CpGpCpGpCpG) and d(CpGpCpG) (1–4) and fibers of the polymer (dG-dC)$_n$·(dG-dC)$_n$ (5). The observation of left-handed conformations for dC-dG sequences helped resolve questions concerning the unusual solution properties of (dG-dC)$_n$·(dG-dC)$_n$. It has been known for some time that spectroscopic properties of (dG-dC)$_n$·(dG-dC)$_n$ show major changes with increasing ionic strength (6). In low salt solutions (<2.0 M NaCl), circular dichroic spectra (7, 8) and Raman spectra (9) are characteristic of a B-type DNA. Increased concentrations of salts or ethanol induce an inversion of the circular dichroic spectrum and changes of the Raman spectrum indicative of a cooperative intramolecular transition (8–10). The Raman spectrum of the Z conformation crystal of d(CpGpCpGpCpG) is essentially identical to the spectrum of (dG-dC)$_n$·(dG-dC)$_n$ in high salt solutions (11). This correlation together with nuclear magnetic resonance studies (12, 13) indicate that the high salt form of (dG-dC)$_n$·(dG-dC)$_n$ is a Z-type conformation.

Recent studies have shown that dC-dG regions can exist in a left-handed conformation when joined to a natural DNA segment. Recombinant DNA techniques were used to construct a 157-base pair (bp) restriction fragment that contains a 95-bp segment of the *Escherichia coli lac* operator–promoter region (14) flanked between 26 and 32 bp of dC-dG sequences (15). Fig. 1 illustrates the DNAs used in this study. The "157-bp fragment" has 153 duplex bp and the "95-bp fragment" has 95 duplex bp. Both fragments have four nucleotide tails. Circular dichroism and ^{31}P nuclear magnetic resonance studies have shown that a portion of this DNA exists in a Z-type conformation in 4.5–5.0 M NaCl solution. This and other results demonstrated that a junction can occur between a DNA region in a Z-type conformation and an adjacent region that normally assumes a B-type conformation (15).

In the present study Raman spectroscopy was employed to examine the 95-bp *lac* fragment, the 157-bp fragment, and (dG-dC)$_n$·(dG-dC)$_n$ in 0.01 and 4.5 M NaCl. Raman spectra of the 95-bp fragment show bands characteristic of a B-type ($\overline{B}$) conformation in both low and high salt solutions. Raman spectra of the 157-bp fragment in 0.01 M NaCl are also characteristic of $\overline{B}$ DNA. In 4.5 M NaCl, major changes occur in the spectrum of the 157-bp fragment. These changes are the same as the spectral changes observed for (dG-dC)$_n$·(dG-dC)$_n$ and confirm the presence of $\overline{Z}$ conformation in this fragment. A quantitative comparison was made between the 157-bp fragment spectra and spectra calculated from the 95-bp fragment and (dG-dC)$_n$·(dG-dC)$_n$. The observed intensities of bands at 682 cm^{-1} and 627 cm^{-1} indicate that in 4.5 M NaCl essentially all of the dC-dG regions of the 157-bp DNA are in the $\overline{Z}$ conformation. Intensity predicted at 835 cm^{-1} is not observed. The latter band has been correlated with a ribose phosphate vibration in the $\overline{B}$ conformation (16–18). Absence of intensity indicates that a substantial portion (80% ± 15%; ±SD) of the 95-bp segment in the 157-bp fragment is distorted by the left-handed helical ends. This distortion is not indicated by a comparison of calculated and observed intensities of base vibrations at 682 cm^{-1}, 730 cm^{-1}, and 750 cm^{-1}.

MATERIALS AND METHODS

Raman Instrumentation. The Raman spectroscopy system employs digital photon counting and is controlled by a PDP-8f computer. A general description of the system has been given previously (19). All Raman spectra were obtained with the 514.5-nm line of an argon ion laser. Laser power of 180–300 mW was used to record spectra from 400 to 1935 cm^{-1}. The laser beam was focused up into the liquid sample that was contained in fused quartz cells that were 2 mm in diameter. Cells contained 10–15 μl of DNA solution or solvent and were capped. All Raman spectra are the sum of three to five consecutive scans. Each scan accumulated counts for 1 sec/cm^{-1}. The temperature was ≈24°C.

The publication costs of this article were defrayed in part by page charge payment. This article must therefore be hereby marked "*advertisement*" in accordance with 18 U. S. C. §1734 solely to indicate this fact.

Abbreviation: bp, base pair(s).

‡ Present address: Institut für Organische Chemie und Biochemie, Technische Hochshule-Darmstadt, 6100 Darmstadt, Federal Republic of Germany.

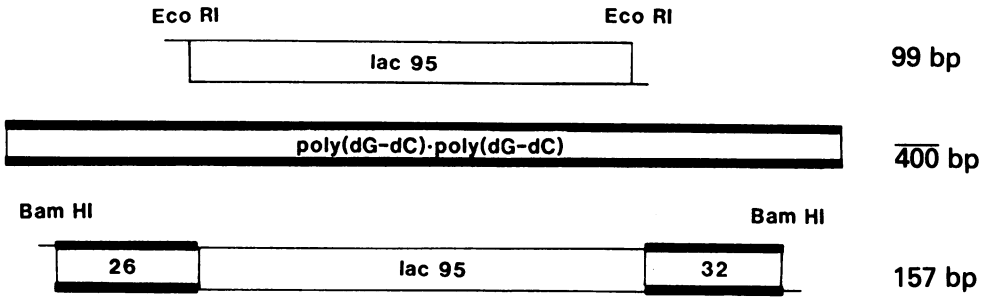

FIG. 1. Three DNAs employed in this study. The 95-bp fragment is the *Alu* I fragment of the *E. coli* lactose operator–promoter region (14) with four base *Eco*RI ends. Including these ends, it has 99 bp. It is referred to as the 95-bp fragment to be consistent with previous descriptions. $(dG\text{-}dC)_n\cdot(dG\text{-}dC)_n$ was about 400 bp long. The 157-bp fragment contains the 95-bp region flanked by G-C regions and *Bam*HI ends.

DNAs. The DNA polymer $(dG\text{-}dC)_n\cdot(dG\text{-}dC)_n$ was purchased from P-L Biochemicals. It was extracted with phenol prior to Raman experiments. Its sedimentation coefficient indicated an average size of ≈400 bp. Preparation and characterization of the 95-bp and 157-bp DNA fragments have been described (14, 15, 20). DNA samples were prepared for Raman spectroscopy by precipitating 1–2 mg of DNA with ethanol in a 1.5-ml tube. The DNAs were pelleted by centrifugation for 4 min at 13,000 × *g* and were washed several times with 80% ethanol at 4°C. They were then lyophilized to dryness. Samples were dissolved to concentrations of 20–40 mg/ml by addition of 0.01 or 4.5 M NaCl solutions. DNA concentrations were measured by diluting 2 μl in 1.0 ml of 0.01 M NaCl solvent. The following extinction coefficients were used: 95-bp fragment, $6.5 \times 10^3\ M^{-1}\cdot cm^{-1}$; $(dG\text{-}dC)_n\cdot(dG\text{-}dC)_n$, $7.1 \times 10^3\ M^{-1}\cdot cm^{-1}$; 157-bp fragment, $6.7 \times 10^3\ M^{-1}\cdot cm^{-1}$ (15).

Data Analysis. Two methods were examined for background subtraction under the DNA spectra. In the first method, the computer subtracted various amounts of the Raman spectra of the solvents (19). Although this method generally gave a flat background, the curvature of the solvent Raman spectrum did not always follow the DNA spectra background. To provide a consistent subtraction procedure, a second method was developed that fit a continuous curve to the background of a Raman spectrum (unpublished).

A typical example of a DNA spectrum and its fitted background curve is shown in Fig. 2. Least squares polynomial curves (up to third order) were fit to unambiguous background regions and continuously connected to background points. These points were determined from a computer-generated list of valley points from original DNA spectra and an examination of solvent spectra. This method did not add any noise to DNA spectra and provided a consistent subtraction procedure for all DNA spectra. The first subtraction method—although not used in the analyses—provided a valuable check for the computer-generated background method. When comparisons were possible, both methods gave very similar results. DNA spectra with flattened backgrounds were then smoothed by a least squares fit of third-order polynomials to overlapping 15-point regions (21). This procedure was very effective in decreasing noise without flattening or distorting peaks.

Figs. 3, 4, and 5 show the smoothed spectra of $(dG\text{-}dC)_n\cdot(dG\text{-}dC)_n$, the 95-bp DNA, and the 157-bp DNA, respectively. The Raman spectra of the 157-bp DNA was compared to the spectra calculated from the 95-bp DNA and $(dG\text{-}dC)_n\cdot(dG\text{-}dC)_n$. This required normalization of the spectra to the same relative scattering power, DNA concentration, and molar ratio of nucleotides of the dC-dG and 95-bp regions in the 157-bp fragment.

The water band at 1645 cm^{-1} was used as an internal standard

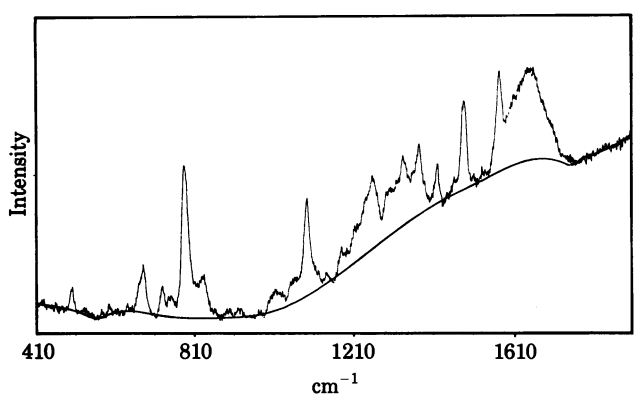

FIG. 2. Original Raman spectrum of the 157-bp fragment in 0.01 M NaCl. The background curve was generated as described.

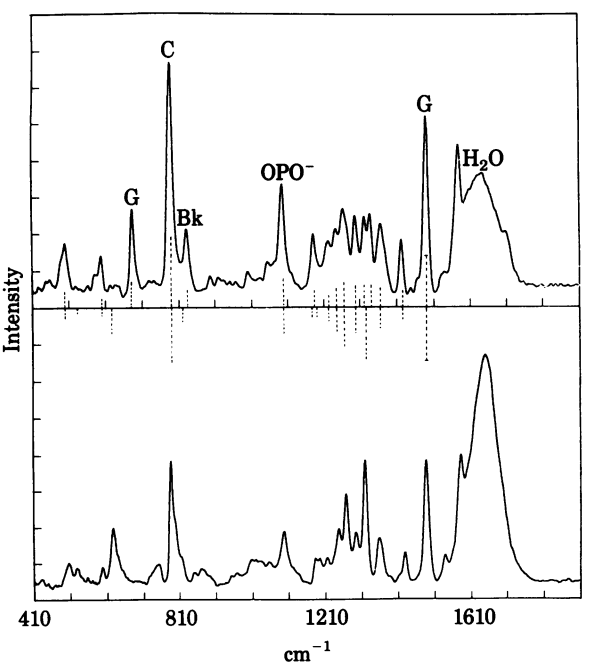

FIG. 3. Smoothed Raman spectra of $(dG\text{-}dC)_n\cdot(dG\text{-}dC)_n$ after background subtraction. Assignments of several peaks are shown: G, guanine; C, cytosine; Bk, backbone; OPO^-, dioxy stretch. Dashed lines above and below the midline correspond to peak intensities in 0.01 M (*Upper*) and 4.5 M (*Lower*) NaCl, respectively, relative to the 1488-cm^{-1} band. This band is normalized to 1 in both spectra. Comparison of these spectra by using Na_2SO_4 as an independent internal standard indicated a slight decrease in the 1488-cm^{-1} intensity at the higher salt concentration.

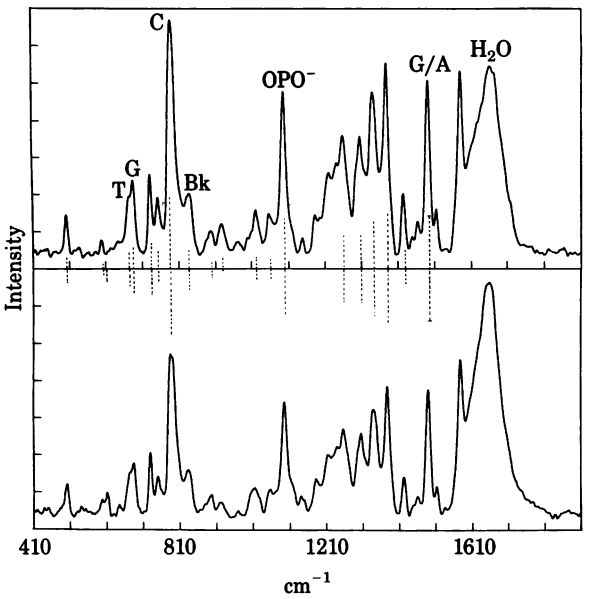

FIG. 4. Smoothed Raman spectra of the 95-bp fragment after background subtraction. Assignments are the same as in Fig. 3, with the additions: T, thymine and G/A, guanine and to a lesser extent adenine. Dashed lines are intensities normalized relative to the 1488-cm^{-1} band. (*Upper*) 0.01 M NaCl; (*Lower*) 4.5 M NaCl.

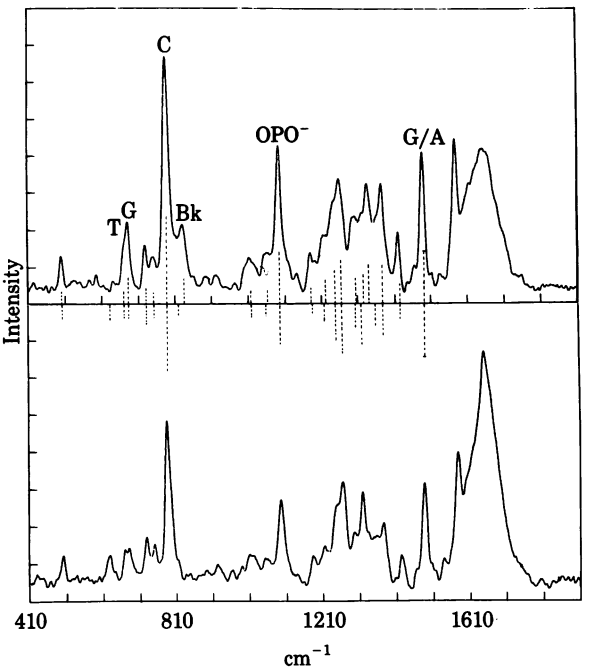

FIG. 5. Smoothed Raman spectra of the 157-bp fragment after background subtraction. (*Upper*) 0.01 M NaCl; (*Lower*) 4.5 M NaCl. See Figs. 3 and 4 for other information.

for the combination of experimental factors that affect scattering power (e.g., laser power, optical alignment, counting time). A test of the normalization for scattering power and DNA concentration was made by comparing three Raman spectra of the 95-bp fragment taken at different DNA concentrations and laser power. Peak intensities for all medium to large peaks were within ± 10% (±SD) of one another. Calculated Raman spectra of the 157-bp DNA were made from experimental spectra of $(dG\text{-}dC)_n\cdot(dG\text{-}dC)_n$ and the 95-bp DNA by using the following equation

$$I^{\bar{\nu}}_{157} = \frac{P_{157}C_{157}}{P_{GC}C_{GC}}\left(\frac{58}{153}\right) I^{\bar{\nu}}_{GC} + \frac{P_{157}C_{157}}{P_{95}C_{95}}\left(\frac{95}{153}\right) I^{\bar{\nu}}_{95}. \quad [1]$$

$I^{\bar{\nu}}_{157}$ is the calculated Raman intensity of the 157-bp DNA at wavenumber $\bar{\nu}$ that is calculated from a sum of the normalized intensities of $(dG\text{-}dC)_n\cdot(dG\text{-}dC)_n$ and the 95-bp fragment. It is comparable to an experimental intensity measured from a sample at a molar concentration of C_{157} in nucleotides and with P_{157} as the intensity of the 1645-cm^{-1} water band. $I^{\bar{\nu}}_{GC}$ and $I^{\bar{\nu}}_{95}$ correspond to the experimental Raman intensities at wavenumber $\bar{\nu}$ of $(dG\text{-}dC)_n\cdot(dG\text{-}dC)_n$ and the 95-bp fragment, respectively. They are measured from samples at concentrations C_{GC} and C_{95} and with water band intensities of P_{GC} and P_{95}, respectively. The four nucleotide long "tails" are neglected in Eq. 1.

RESULTS

Raman spectra of $(dG\text{-}dC)_n\cdot(dG\text{-}dC)_n$ in 0.01 M and 4.5 M NaCl are shown in Fig. 3. The low salt spectrum has bands characteristic of DNAs in the $\overline{B}$ conformation (16, 17). In particular, one observes a band at 832 cm^{-1}—assigned to a ribose phosphate vibration (18)—and the 682-cm^{-1} peak—associated with the guanine ring (22–24). The large peak at 784 cm^{-1} is assigned to a cytosine ring vibration (22). A backbone vibration centered at ≈795 cm^{-1} contributes to the right shoulder of this peak. This is not discernable on the scale of this figure, but it can be detected upon expanding this region (25). The large 1488-cm^{-1} peak is assigned to a guanine ring vibration (22, 24) and the 1095-cm^{-1} band is assigned to a symmetric dioxy PO_2^- vibration (17, 22). The $(dG\text{-}dC)_n\cdot(dG\text{-}dC)_n$ spectrum in 4.5 M NaCl is essentially identical to that previously observed (9) and is correlated with the $\overline{Z}$ conformation (11). It is characterized by the disappearance of intensity at 682 cm^{-1} and at 832 cm^{-1}. New bands appear at 627 cm^{-1} and 730 cm^{-1}. Two shoulders are now observed on the right side of the 784-cm^{-1} peak at 795 cm^{-1} and 815 cm^{-1}. Large intensity changes also occur between 1230 and 1350 cm^{-1}.

Fig. 4 shows the Raman spectra of the 95-bp *lac*-operon fragment in 0.01 and 4.5 M NaCl. The low salt spectrum shows an 835-cm^{-1} vibration characteristic of $\overline{B}$ DNA. A peak at 669 cm^{-1}—assigned to thymine (22)—forms a shoulder to the 682-cm^{-1} guanine vibration. Other bands are similar to those observed for calf thymus DNA in the $\overline{B}$ conformation (22, 25). The 95-bp fragment spectrum in 4.5 M NaCl shows some intensity changes between 550 and 600 cm^{-1} and 750 and 950 cm^{-1}. However, the spectrum remains characteristic of $\overline{B}$ DNA.

Raman spectra of the 157-bp fragment are shown in Fig. 5. The low salt spectrum is indicative of a $\overline{B}$-DNA conformation. An 835-cm^{-1} backbone vibration is observed. As expected, the guanine band at 682 cm^{-1} has a greater intensity relative to the 669-cm^{-1} band than observed for the 95-bp DNA. The Raman spectrum of the 157-bp fragment in 4.5 M NaCl shows a new band at 627 cm^{-1}. In addition, decreases in intensity are observed at 682 cm^{-1} and at 835 cm^{-1}. A shoulder at 815 cm^{-1} is observed. These changes as well as the increased intensity at 1322 cm^{-1} and alterations in the 1200–1300-cm^{-1} region clearly indicate the presence of a $\overline{Z}$ conformation in the 157-bp fragment. These results confirm the circular dichroism and ^{31}P nuclear magnetic resonance studies (15).

The Raman spectra of the 157-bp DNA were compared to the spectra calculated from the 95-bp DNA and $(dG\text{-}dC)_n\cdot(dG\text{-}dC)_n$. In 0.01 M NaCl—in which all DNAs are in a $\overline{B}$ conformation—a comparison of the spectra tests the assumption of Eq. 1 and the normalization procedure. Fig. 6*A* compares actual and calculated spectra of the 157-bp fragment in 0.01 M NaCl. The calculated spectrum is 0.96 of the value determined from Eq. 1.

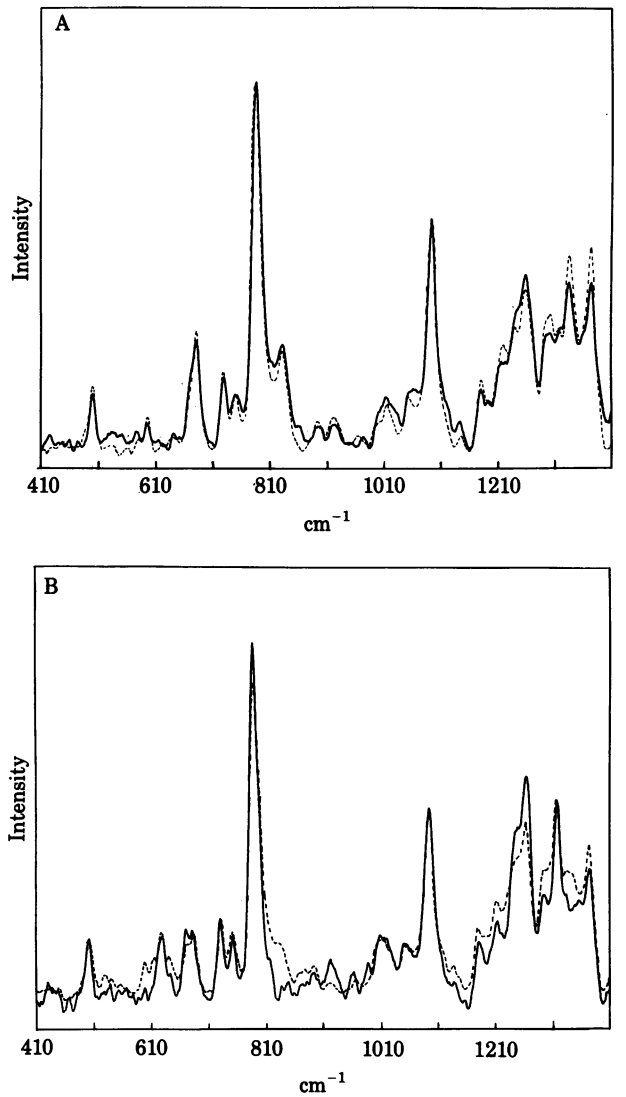

FIG. 6. (*A*) Comparison of experimental (——) Raman spectra of 157-bp fragment with spectrum calculated (----) from 95-bp fragment and $(dG\text{-}dC)_n\cdot(dG\text{-}dC)_n$ in 0.01 M NaCl. (*B*) Comparison of experimental (——) and calculated (----) spectra of 157-bp fragment in 4.5 M NaCl.

This adjustment normalized peak heights of the 1095-cm^{-1} band. It is within expected error. Close agreement is observed for the two spectra. All calculated peak intensities from 400 to 1300 cm^{-1} are within ± 10% (±SD) of experimental peak heights. The predicted intensities of peaks at 1300 cm^{-1}, 1336 cm^{-1}, and 1378 cm^{-1} are all somewhat higher than actual peak heights (10–16%). This is probably due to inaccuracies in determination of background curves in this region.

Fig. 6*B* shows the experimental and calculated spectra of the 157-bp DNA in 4.5 M NaCl. The calculated spectrum presumes that all of the dC-dG regions of the 157-bp DNA are in the $\overline{Z}$ conformation and that the 95-bp region is in the $\overline{B}$ conformation. As in the previous comparison, there is close overall agreement between calculated and experimental spectra. The intensities of the 500-cm^{-1} band and the symmetric dioxy PO_2^- stretch vibration at 1095 cm^{-1} are accurately predicted. The 627-cm^{-1} and 682-cm^{-1} bands are also closely predicted. These two bands are sensitive to the conformation of the dC-dG regions (Fig. 3). The agreement between the calculated and observed intensities of these bands indicates that essentially all

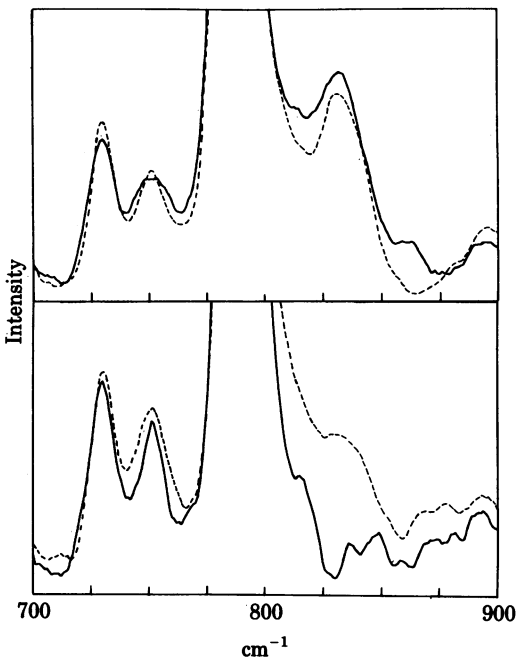

FIG. 7. Comparison of experimental (——) and calculated (----) Raman spectra of the 157-bp fragment for the 650–900-cm^{-1} regions of Fig. 6. (*Upper*) 0.01 M NaCl; (*Lower*) 4.5 M NaCl.

of the dC-dG segments are in the $\overline{Z}$ conformation. This agrees with the ^{31}P nuclear magnetic resonance measurements of the 157-bp DNA but differs from determinations based on circular dichroism (15). Fig. 7 shows enlargements of the 650–900-cm^{-1} regions of Fig. 6 *A* and *B*. Fig. 7 *Lower* shows that the high salt spectrum of the 157-bp fragment has much less intensity at 835 cm^{-1} than predicted. Comparison with the spectra of Fig. 7 *Upper* as well as other bands in Fig. 7 *Lower* indicates that this difference is significant. This result indicates that a substantial part of the 95-bp segment of the 157-bp fragment is distorted from the $\overline{B}$ conformation. Integrated intensity measurements between 815–850 cm^{-1} show 80% ± 15% (±SD) less intensity in the actual spectrum as compared to that of the calculated spectrum. The error is based on three separate spectra of the DNA fragments, repeated analyses of background subtraction, and normalization. It is worth noting from Figs. 6*B* and 7 *Lower* that some Raman bands assigned to base vibrations are in good agreement with the calculated spectrum. This is observed for the 682-cm^{-1} guanine band, the 730-cm^{-1} band assigned to thymine, and the 750-cm^{-1} adenine band. In addition, some of the peaks from 1200–1900-cm^{-1} that are associated with base vibrations also agree with the calculated spectrum.

Some of the small differences between the calculated and observed spectra in Fig. 6*B* may be due to differences in the background, and it is difficult to assess these variations with confidence. Intensities predicted at 595 cm^{-1}, 610 cm^{-1}, and 645 cm^{-1} are not observed to the same extent in the actual spectra. These bands, although small, are reproducibly observed in the 95-bp DNA and $(dG\text{-}dC)_n\cdot(dG\text{-}dC)_n$ spectra. If their contributions to the predicted intensity of the 627-cm^{-1} band are subtracted, the actual 627-cm^{-1} band appears to have a greater intensity than predicted. Although the significance of this observation is uncertain, it supports the conclusion that essentially all of the dC-dG regions are in the Z conformation.

DISCUSSION

Raman spectroscopy studies have shown that dC-dG regions in the $\overline{Z}$ conformation can distort the conformation of an adjoining

region of natural DNA. Previous studies have also indicated that steric and thermodynamic effects can propagate through DNA (8–10, 26–32). The extent to which a disturbance at one DNA site affects adjoining sites may be expected to depend on the nature of the disturbance and the DNA sequences involved. In addition, detection of a disturbance depends on the experimental probe employed. Observations by several workers (33–35) suggest a possible long-range effect (≈100 bp) involving the interaction of *lac* repressor with its operator DNA site. However, the repressor–operator complex does not appear to affect *Eco*RI cutting 40 bp away (36). The present Raman study indicates a long-range distortion at the junction of $\overline{B}$ and $\overline{Z}$ conformations. Assuming the intensity at 835 cm^{-1} is proportional to the amount of $\overline{B}$ conformation, about 70 bp of the 95-bp region are affected by the dC-dG ends. This observation may have implications with respect to a potential role of $\overline{Z}$ conformation DNA in gene regulation.

The results from this Raman study can be compared to other observations of the $\overline{B}$–$\overline{Z}$ junction (15). Circular dichroic spectra of the 157-bp fragment in high salt showed qualitative but not quantitative agreement. It was concluded from this study that 65% of the dC-dG regions are in a $\overline{Z}$ conformation, 10 bp of each dC-dG region are in a non-$\overline{Z}$ conformation, and most of the 95-bp segment is in a $\overline{B}$ structure. However, evaluation of ^{31}P nuclear magnetic resonance studies indicated that virtually all of the dC-dG regions are in a $\overline{Z}$ conformation in high salt. Results from high-salt agarose gel electrophoresis of fractionated plasmid DNA topoisomers that contain the 157-bp fragment indicated a junction region of a few base pairs (unpublished). The differences in the conclusions from these studies may be more apparent than real because different conformational features of the junction are being examined.

The conformation of the middle portion of the 157-bp fragment in high salt is uncertain. Natural DNAs and a number of synthetic DNAs [$d(A)_n \cdot d(T)_n$, $(dA\text{-}dT)_n \cdot (dA\text{-}dT)_n$, $d(G)_n \cdot d(C)_n$, $d(G\text{-}C)_n \cdot d(G\text{-}C)_n$] all show a Raman band peaking between 830 and 840 cm^{-1} in low salt solutions (ref. 22; also unpublished). Studies from x-ray diffraction analyses (37) and gel electrophoresis (38, 39) suggest that in low salt solutions these DNAs are in the $\overline{B}$ conformation family, with variations about an average structure occurring for some of the DNA sequences. Because all of these DNAs show an 830–840-cm^{-1} band, absence of intensity in this region implies a conformation which is no longer in the $\overline{B}$ family. Whether the conformation of the junction region is one conformation or a continuum of conformations cannot be determined. The change in the ribose phosphate vibration of the 157-bp fragment is not reflected by similar changes in a number of Raman bands associated with base vibrations. Raman bands at 682 cm^{-1}, 730 cm^{-1}, and 750 cm^{-1} show intensity changes upon undergoing a $\overline{B}$ to $\overline{Z}$ or $\overline{B}$ to $\overline{A}$ transition (or both) (17, 25). The intensities of these bands are accurately predicted by assuming the 95-bp region is in its high salt $\overline{B}$ conformation and the dC-dG regions are in the $\overline{Z}$ conformation. This observation suggests that the base pair stacking of the 95-bp region is not altered to the extent indicated for the ribose phosphate backbone. This is consistent with the circular dichroism studies that indicated that most of the 95-bp region remained in the $\overline{B}$ conformation.

The authors thank P. O'Rourke and C. Mudare for their help in maintaining the Raman instrumentation. Support for this work is gratefully acknowledged from the National Institutes of Health (AI16874 and CA20279) and National Science Foundation (PCM77-15033). R.M.W. is a recipient of a Research Career Development Award from the National Institutes of Health.

1. Wang, A. H., Quigley, G. J., Kolpak, F. J., Crawford, J. L., van Boom, J. H., Van der Marel, G. & Rich, A. (1979) *Nature (London)* **282**, 680–686.
2. Crawford, J. L., Kolpak, F. J., Wang, A. H.-J., Quigley, G. J., van Boom, J. H., Van der Marel, G. & Rich, A. (1980) *Proc. Natl. Acad. Sci. USA* **77**, 4016–4020.
3. Wang, A. H.-J., Quigley, G. J., Kolpak, F. J., Van der Marel, G., van Boom, J. H. & Rich, A. (1981) *Science* **211**, 171–176.
4. Drew, H., Takano, T., Tanaka, S., Itakura, K. & Dickerson, R. E. (1980) *Nature (London)* **286**, 567–573.
5. Arnott, S., Chandrasekaran, R., Birdsall, D. L., Leslie, A. G. W. & Ratliff, R. L. (1980) *Nature (London)* **283**, 743–745.
6. Wells, R. D., Goodman, T. C., Hillen, W., Horn, G. T., Klein, R. D., Larson, J. E., Müller, U. R., Neuendorf, S. K., Panayotatos, N. & Stirdivant, S. M. (1980) *Prog. Nucleic Acids Res. Mol. Biol.* **24**, 167–267.
7. Wells, R. D., Larson, J. E., Grant, R. C., Shortle, B. E. & Cantor, C. R. (1970) *J. Mol. Biol* **54**, 465–497.
8. Pohl, F. M. & Jovin, T. M. (1972) *J. Mol. Biol.* **67**, 375–396.
9. Pohl, F. M., Ranade, A. & Stockburger, M. (1973) *Biochim. Biophys. Acta* **335**, 85–92.
10. Pohl, F. M. (1976) *Nature (London)* **260**, 365–366.
11. Thamann, T. J., Lord, R. C., Wang, A. H.-J. & Rich, A. (1981) *Nucleic Acids. Res.* **9**, 5443–5457.
12. Patel, D. J., Canuel, L. L. & Pohl, F. M. (1979) *Proc. Natl. Acad. Sci. USA* **76**, 2508–2511.
13. Simpson, R. T. & Shindo, H. (1980) *Nucleic Acids Res.* **8**, 2093–2103.
14. Hardies, S. C., Patient, R. K., Klein, R. D., Ho, F., Reznikokk, W. S. & Wells, R. D. (1979) *J. Biol. Chem.* **254**, 5527–5534.
15. Klysik, J., Stirdivant, S., Larson, J. E., Hart, P. A. & Wells, R. D. (1981) *Nature (London)* **290**, 671–677.
16. Erfurth, S. C., Kiser, E. J. & Peticolas, W. L. (1972) *Proc. Natl. Acad. Sci. USA* **69**, 938–941.
17. Erfurth, S. C., Bond, P. & Peticolas, W. L. (1975) *Biopolymers* **14**, 1245–1257.
18. Lu, K. C., Prohofsky, E. W. & Van Zandt, L. L. (1977) *Biopolymers* **16**, 2491–2506.
19. Martin, J. C., Wartell, R. M. & O'Shea, D. C. (1978) *Proc. Natl. Acad. Sci. USA* **75**, 5483–5487.
20. Hillen, W., Klein, R. D. & Wells, R. D. (1981) *Biochemistry* **20**, 3748–3756.
21. Savitzky, A. & Golay, M. J. (1964) *Anal. Chem.* **36**, 1627–1638.
22. Erfurth, S. C. & Peticolas, W. L. (1975) *Biopolymers* **14**, 247–264.
23. Lafleur, L., Rice, J. & Thomas, G. J., Jr. (1972) *Biopolymers* **11**, 2423–2431.
24. Lord, R. C. & Thomas, G. J., Jr. (1967) *Spectrochim. Acta* **23**, 2551–2557.
25. Martin, J. C. & Wartell, R. M. (1982) *Biopolymers*, in press.
26. Burd, J. F., Wartell, R. M., Dodgson, J. B. & Wells, R. D. (1975) *J. Biol. Chem.* **250**, 5109–5113.
27. Burd, J. F., Larson, J. E. & Wells, R. D. (1975) *J. Biol. Chem.* **250**, 6002–6007.
28. Wartell, R. M. & Burd, J. F. (1976) *Biopolymers* **15**, 1461–1479.
29. Hogan, M., Dattagupta, N. & Crothers, D. M. (1979) *Nature (London)* **278**, 521–524.
30. Patel, D. J. & Canuel, L. L. (1977) *Proc. Natl. Acad. Sci. USA* **74**, 5207–5210.
31. Selsing, E., Wells, R. D., Early, T. A. & Kearns, D. R. (1978) *Nature (London)* **275**, 249–250.
32. Selsing, E., Wells, R. D., Alden, C. & Arnott, S. (1979) *J. Biol. Chem.* **254**, 5417–5422.
33. Chan, H. W. & Wells, R. D. (1974) *Nature (London)* **252**, 205–208.
34. Sadler, J. R., Tecklenburg, M. & Betz, J. L. (1980) *Gene* **8**, 279–287.
35. Winter, R. B. & von Hippel, P. H. (1981) *Biochemistry* **20**, 6948–6960.
36. Frankel, A. D. & Smith, H. O. (1981) *J. Mol. Biol.* **146**, 611–619.
37. Leslie, A. G. W., Arnott, S., Chandrasekaran, R. & Ratliff, R. L. (1980) *J. Mol. Biol.* **143**, 49–72.
38. Peck, L. J. & Wang, J. C. (1981) *Nature (London)* **292**, 375–378.
39. Rhodes, D. & Klug, A. (1981) *Nature (London)* **292**, 378–380.